THE STUDY OF RADAR ABSORBING STRUCTURES FOR WIND POWER TURBINE BLADES

Hong K. Jang, Won J. Lee, Sang E. Lee, Chun G. Kim and Jin B. Kim
School of Mechanical, Aerospace and Systems Engineering, Division of Aerospace Engineering, KAIST
373-1 Guseong-dong, Yuseong-gu, Daejeon, 305-701, Republic of Korea

Summary

The large radar cross section and high tip speeds of wind turbine blades can affect radar systems used for air traffic control, marine navigation, weather monitoring and the military. In this study, we show an electromagnetic wave absorbing composite structure to solve radar problems. This technology will allow blades to absorb radar signals without compromising their structural strength, while reducing or eliminating reflected wave. First, the double-layered radar absorbing structures (RAS) including a frequency selective fabric composite (FSFC) with broadband absorption was developed. The FSFC was proposed consisting of carbon and low-loss dielectric fibers and the two layers were made by MWNT-added glass / epoxy plain-weave composites. Second, thin and ultra-wide band RAS with a periodic square patterned conducting polymer layer was fabricated. To make the periodic pattern layer, the intrinsic conducting polymer based on the poly(ethylenedioxy)thiophene (PEDOT) was synthesized. The RAS consisting of fiber reinforced composites is expected to carry loads and also absorb electromagnetic waves.

KEY WORDS: Composite Turbine Blades, Radar Cross Section, Doppler, Radar Absorbing Structures, Stealth Blades

1. INTRODUCTION

Renewable energy resources are the solution to the problems of global warming and the finite reserves of fossil fuels. Especially wind energy is a fast growing market worldwide. But the large radar cross section and high tip speeds of wind turbine blades can affect radar systems used for air traffic control, marine navigation, weather monitoring and the military. Thus a number of proposed wind

farm projects have been stopped and cancelled in the world [1~2]. The purpose of this paper is to present the new radar absorbing structures for wind turbine blades made by composite materials and to show the possibility of developing stealth blades.

Radar cross section (RCS) reduction technology for structures such as turbine blades is categorized into the shape design, radar absorbing materials (RAM) and radar absorbing structures (RAS). In general, the RAM are fabricated in the form of sheets consisting of insulating polymer and lossy materials such as ferrites, carbon black, carbon nanotube. They have the advantage of direct application to the surface of structure. But they increase the total weight and have poor mechanical properties, which cannot be used as load bearing structures [3]. On the other hand, the RAS which are composed of fiber reinforced composites and lossy fillers in the matrix can be used as a load bearing structure with EM wave absorbing characteristics [4].

2. MULTI-LAYERED RAS USING MWNT

2.1 MWNT-filled glass/epoxy composite

In this study, MWNTs and glass/epoxy plain-weave composites were used for radar absorbing structures. First, the MWNTs were dispersed in epoxy matrix. The fabric composites were impregnated by the mixture of the matrix and the MWNTs. The weight fraction of MWNTs to the total weight of the fabric, the epoxy system and the MWNTs are shown in Table 2.1.1.

Table 2.1.1 Denotation of MWNT-filled glass/epoxy composites

Denotation	MWNT 0.0	MWNT 0.4	MWNT 0.7
Content (wt%)	0.0	0.4	0.7

Denotation	MWNT 1.0	MWNT 1.3	MWNT 1.6
Content (wt%)	1.0	1.3	1.6

The microstructure of the fabricated composites was captured by scanning electron microscopy (SEM). Figure 2.1.1 shows the images of interface between the glass fiber yarns in the warp and fill directions of MWNT 1.0.

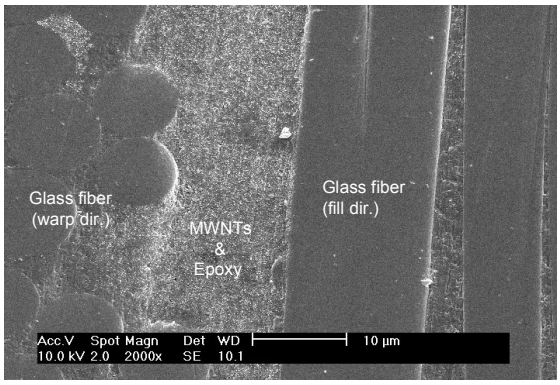

Fig. 2.1.1 SEM image of MWNT 1.0

Five specimens per MWNT content were used to measure permittivity, as shown in Fig. 2.1.2. This figure revealed that the permittivities of all the specimens were nearly constant, regardless of frequency, and that they increased exponentially with the weight fraction of MWNT [5].

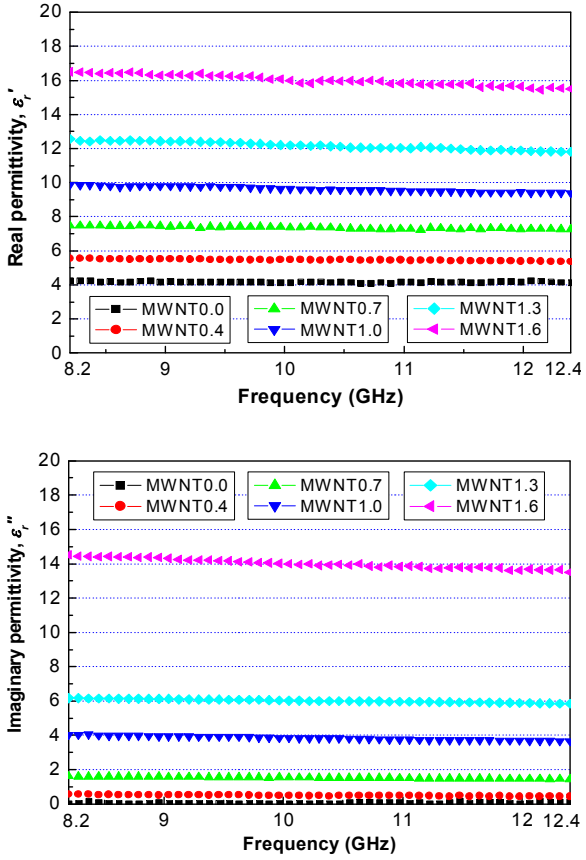

Fig. 2.1.2 Relative permittivity of MWNT-filled composites with frequency

2.2 Double-layered RAS using MWNT

Optimal design algorithm was established by linking a genetic algorithm (GA) with a reflection loss analysis of multi-layered RAS [5]. The thickness and permittivity of each layer were selected as design variables.

The optimal design was performed for a two-layered RAS. The thickness to be simulated was limited to 3.5 mm. The back surface of the RAS was assumed to be a perfect conductor. The RAS design with the largest absorption bandwidth was composed of MWNT 0.4, with a thickness of 1.9 mm, and MWNT 1.6, with a thickness of 1.4 mm. The reflection loss of this RAS is shown in Fig. 2.21. It had a -10 dB absorbing bandwidth over the entire X-band (8.2 ~ 12.4 GHz), and had a -20 dB absorbing bandwidth of 1.0 GHz.

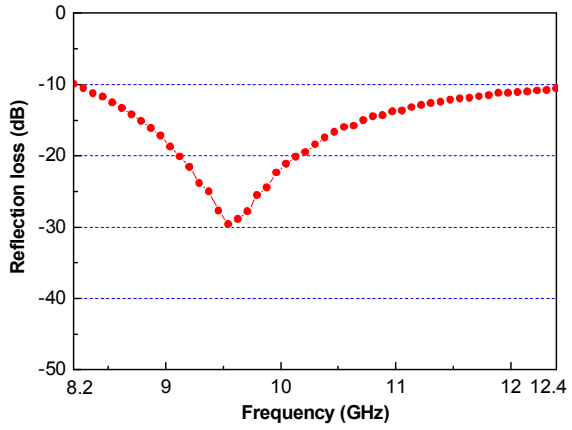

Fig. 2.2.1 Reflection loss of the optimal RAS design

According to Table 2.2.1, the designed RAS was expected to have a thickness of 3.29 mm by using 13 plies for MWNT 0.4 (1.94 mm) and 9 plies for MWNT 1.6 (1.35 mm). However, the fabricated RAS had a thickness of 3.27 mm, which has only 0.02 mm thickness difference compared to the predicted thickness of 3.29 mm.

Table 2.2.1 Ply thickness according to the number of plies and MWNT contents

Material	No. of plies	Thick. (mm)	Thick. / ply (mm)
MWNT 0.4	21	3.28	0.149
MWNT 1.6	20	3.38	0.169

The analytical and experimental reflection loss and the resonant frequency of the RAS are shown in Fig. 2.2.2. The results were found to be in good agreement with the analytical results. It had a -10 dB absorbing bandwidth from 8.3 GHz to 11.6 GHz and resonant frequency of 9.8 GHz.

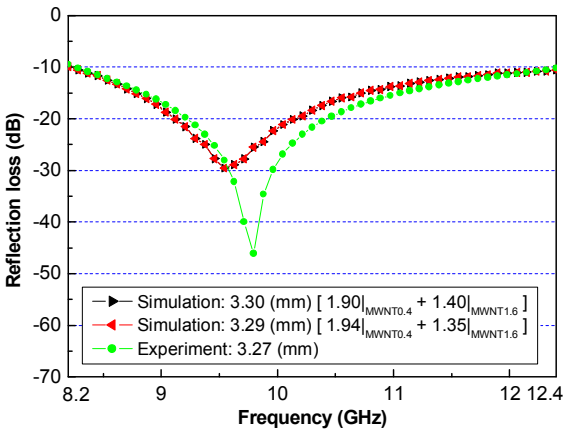

Fig. 2.2.2 Comparison of reflection loss between simulation and experiment

3. COMPOSITE RAS INCLUDING FSFC

3.1 Fabrication of FSFC

In general, frequency selective surface (FSS) was composed of metal, such as copper or aluminum. It was fabricated by chemical etching of a metal-coated thin film. The FSS can also be composed of carbon fiber and low-loss dielectric fiber, such as E-glass. The carbon fibers reflect incident waves due to the high electrical conductivity, corresponding to metal part in an FSS, and the low-loss dielectric fibers transmit most of the incident waves, corresponding to aperture part. Therefore the proposed FSFC can be used as an inductive FSS [6].

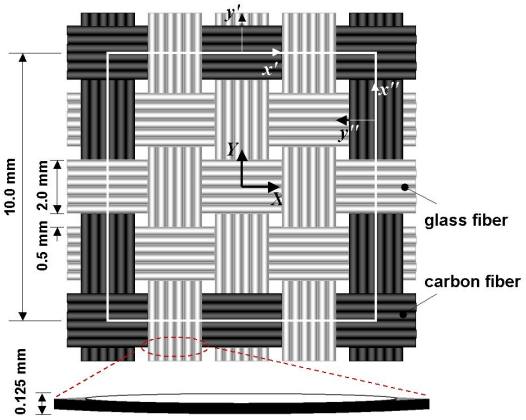

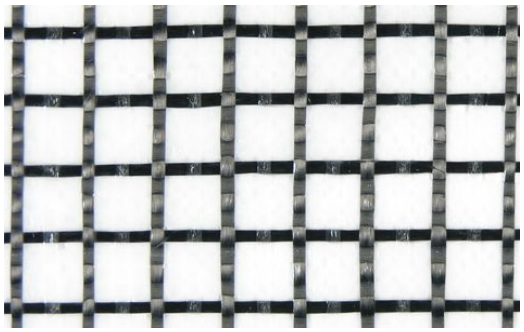

Fig. 3.1.1 Schematic of a fabricated FSFC

In this study, the FSFC was fabricated as a plain-weave type with square elements in a cell size of 10 mm and an aperture size of 8 mm. T300 and E-glass were

used as carbon and dielectric fibers, and an epoxy was selected as matrix. The thickness of the fabricated FSFC was 0.125 mm, illustrated in Fig 3.1.1.

The transmitted power of the FSFC was compared to that of the metallic FSS with an identical cell and aperture size. Figure 3.1.2 shows that the fabricated FSFC function as a high pass filter that reflects most of the low frequency microwave, and that transmits high frequency waves near a resonant frequency. Also the fabricated FSFC had the almost identical or similar transmission coefficients to the metallic FSS.

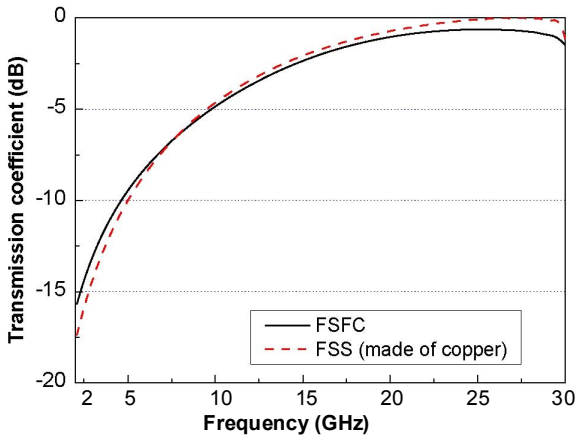

Fig. 3.1.2 Comparison of transmission coefficients of a metallic FSS and FSFC

3.2 FSFC-embedded composite RAS

The FSFC was introduced to modify and improve the absorption performance of a double-layered RAS. The FSFC was also expected to increase the mechanical property of the RAS, because it consists of both carbon and dielectric fibers. Therefore, the developed double-layered composite RAS including a FSFC had not only a broadband absorption performance but also load-carrying ability [6].

The parametric sweeping was conducted with regard to the combination of the dielectric materials (Mat_1, Mat_2), the thickness of each layer (Th_1, Th_2) and the total thickness ($T_{tot} = Th_1+Th_2$) of the RAS not including the FSFC.

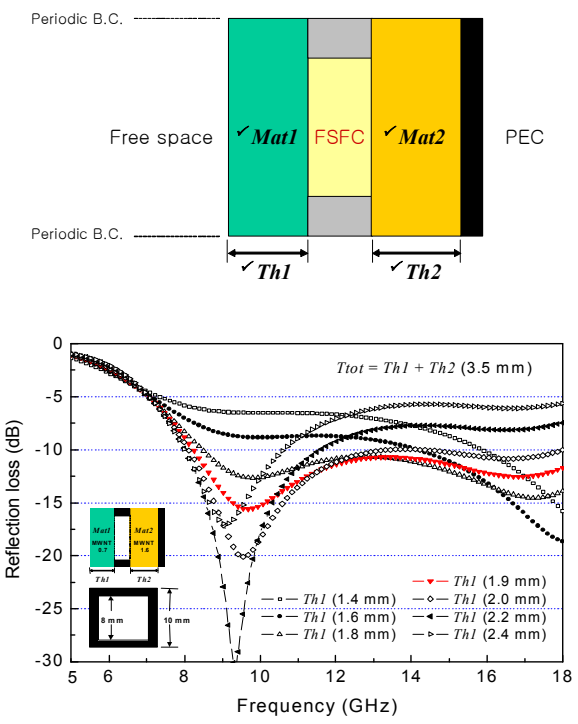

Fig. 3.2.1 Parametric sweeping on the reflection loss of the RAS with a FSFC

According to analytical result, the thinnest FSFC-embedded RAS with the starting frequency of -10 dB absorption at 8.2 GHz was obtained at the T_{tot} of 3.5 mm. The RAS was composed of MWNT 0.7, with a thickness of 1.9 mm, a FSFC with

the cell size 10 mm and the aperture size 8 mm, and MWNT 1.6, with a thickness of 1.6 mm. Its reflection loss is shown in Fig. 3.2.1. The RAS without the FSFC had a -10 dB bandwidth from 6.2 GHz to 8.9 GHz, whereas the RAS with the FSFC showed -10 dB absorption in the whole X- and Ku-band (8.2 ~ 18.0 GHz).

Figure 3.2.2 shows the preparation of the FSFC-embedded RAS before curing. To fabricate the RAS including FSFC with a thickness of 3.625 mm, MWNT 0.7 and MWNT 1.6 was 1.9 mm and 1.6 mm. The RAS was expected to have a thickness of 3.583 mm by using 13 plies for MWNT 0.7 (1.937 mm), 9 plies for MWNT 1.6 (1.521 mm) and 1 ply for the FSFC (0.125 mm). However, the fabricated RAS had a thickness of 3.640 mm, which has 0.057 mm thickness difference.

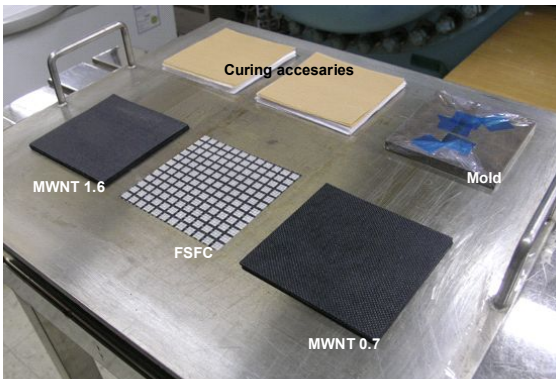

Fig. 3.2.2 Preparation of composite RAS including a FSFC

The analytical and experimental reflection loss and the resonant frequencies of the RAS are shown in Fig. 3.2.3. The results were found to be in good agreement in the whole X-band. The main reasons behind the discrepancy between the analysis and the measurement are as follows: the difference of the electrical conductivity in real and predicted values, the fabrication error, and so on.

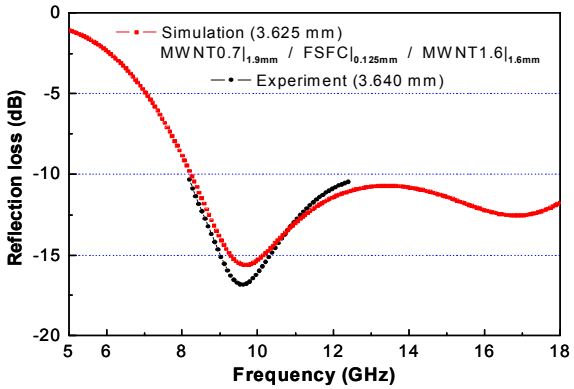

Fig. 3.2.3 Comparison of simulated and measured reflection loss of the best case

4. RAS USING PERIODIC PATTERN

4.1 Design of CP EBG RAS

The electromagnetic bandgap (EBG) that consists of a simple arrangement of unit patterns with highly conductive materials shows EM wave filter characteristics such as the FSS. When the conductivity of the materials for the EBG pattern changes, EM wave absorbing characteristics occur [7]. Especially, conducting polymer (CP) is a promising material for EBG patterns due to its controllable high electric conductivity and simple and effective surface coating, and so on.

In this study, conducting polymer paste

containing PEDOT with polyurethane (binder) was synthesized. The content of PEDOT was 0.6 wt% and the binder was 2.0 wt%; the viscosity of the paste was 5000 cps for the screen printing. The specific conductivity of the CP paste was was 1300 S/m and the conductivity was controlled from 0 ~ 1300 S/m for the EBG pattern application. [8~9]

Based on the principle of the EBG absorber, RLC design and matching can generate radar absorbing characteristics. As the resistance (R) of the EBG pattern can be controlled using the CP paste conductivity and coating thickness, the inductance (L) and capacitance (C) were set at a specific range. In this study, a simple EBG pattern with a square unit cell is considered.

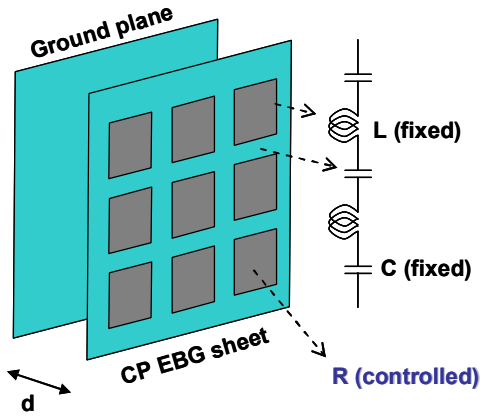

Fig. 4.1.1 Characteristics of EBG layer

The design of RAS with a CP EBG pattern was conducted with parameter sweep and optimization by computational analysis with a 3-D simulator. The final size of unit cell was 10 X 10 mm, the CP pattern was 6 X 6 X 0.012 mm, and the substrate thickness was 2.6 mm. When the thickness approaches to 12 um, the single peak split into two peaks, as shown in Fig. 4.1.2.

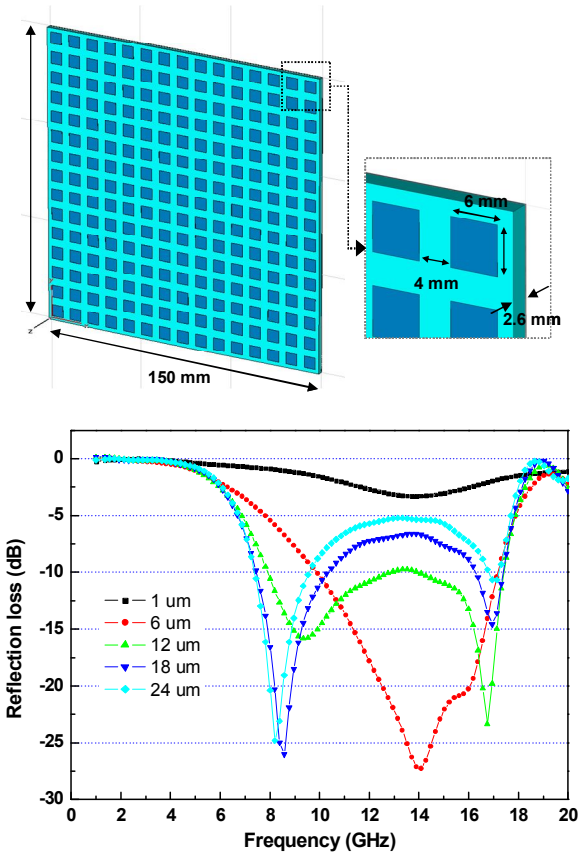

Fig. 4.1.2 Design of EBG pattern layer

4.2 RAS with CP EBG pattern layer

Applying an EBG pattern layer in fiber reinforced composite structures can be effective in designing load bearing RAS with EM wave absorbing characteristics.

First of all, to fabricate the accurate thickness of substrate, thickness per ply (TPP) was calculated. TPP of glass/epoxy plain-weave composites was a thickness

of 0.076 mm, so 34 ply were stacked to make 2.6 mm substrate.

In the second place, the square type metal mask was designed to make the pattern layer on the substrate. The mask was mounted on the screen printer and squeezed the CP paste for printing. The screen printing method used mask and the thickness of the mask can control the coating thickness. As considering the contents of PEDOT and binder in the CP paste, 0.05 mm coating could make approximately 2 um layer on the substrate.

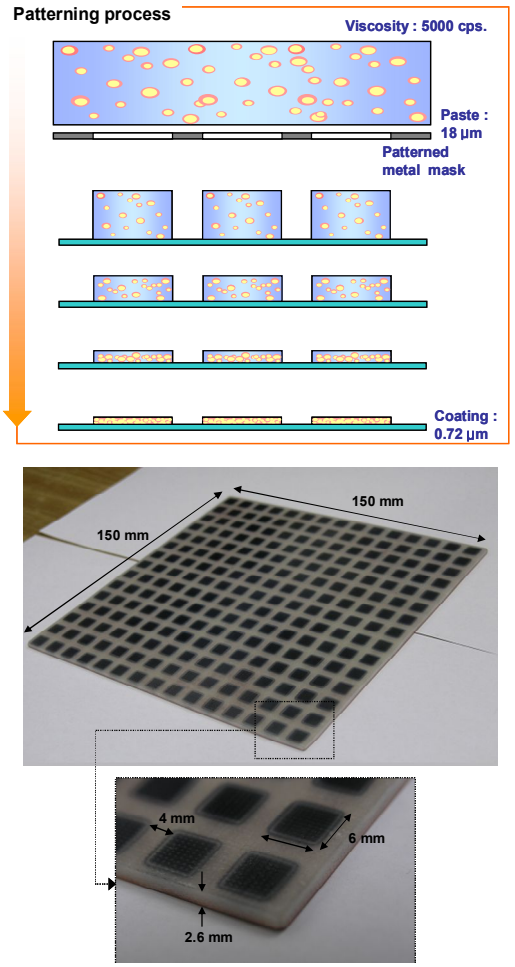

Fig. 4.2.1 CP EBG pattern RAS specimen

Figure 4.2.1 shows the fabricated RAS with CP EBG pattern layer. The radar cross section (RCS) of this absorber was measured using compact range system in anechoic chamber (POSTECH). In this study, the RCS of plate to the oblique incidence angel was measured. The rotation angle of the plate was from -180° to +180°, and the frequency of EM wave was set as 10.3 GHz.

Following Fig. 4.2.2 shows the RCS of copper plate and CP pattern RAS. On the whole direction, the RCS of CP pattern RAS was smaller than that of copper plate. In the case of normal incidence on the plate, the RCS of CP pattern RAS decreased about 11.47 dbsm compared with the copper plate. This means that the RCS of 7.29 m^2 decreased as 0.52 m^2 to the radar system [8~9].

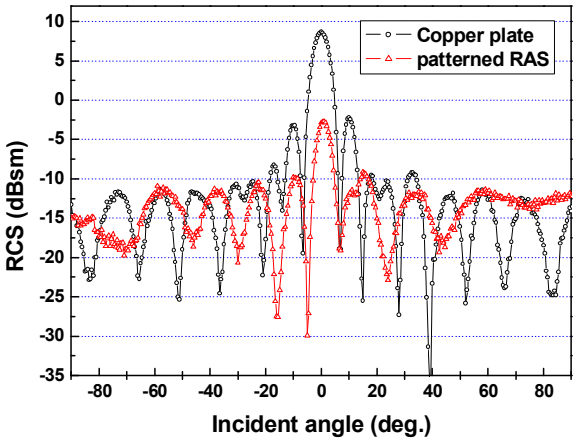

Fig. 4.2.2 RCS of copper plate and CP EBG pattern RAS

5. CONCLUSION

The purpose of this paper is to present the new radar absorbing structures for wind turbine blades and to show the possibility of developing stealth blades.

First, the double-layered RAS using MWNT and including a FSFC were suggested. Second, CP EBS pattern RAS with broadband absorption over a wide frequency range were developed.

To conclude, these technologies will allow blades to absorb radar signals without compromising their structural strength, while reducing or eliminating signals received by radar system.

6. REFERENCES

1. G. J. Poupart, Wind farms impact on radar aviation interests – final report, 2003.
2. M. M. Butlerand, D. A. Johnson, Feasibility of mitigating the effects of windfarms on primary radar, 2003.
3. E. F. knott, J. F. Shaeffer, M. T. Tuley, Radar Cross Section - 2nd, 1993.
4. J. H. Oh, Composites. Part B, Engineering, vol. 35, no. 1, 2004, pp. 49-56.
5. S. E. Lee, J. H. Kang, C. G. Kim, Composite structures, vol. 76, no. 4, 2006, pp. 397-405.
6. S. E. Lee, Ph.D Thesis, Korea Advanced Institute of Science and Technology, 2006.
7. D. J. Kern, D. H. Werner, Microwave and optical technology letters, vol. 38, no. 1, 2003. pp. 61-64.
8. W. J. Lee, J. W. Lee, C. G. Kim, Composite science and technology, vol. 68, no. 12, 2008, pp. 2485-2489.
9. W. J. Lee, Ph.D Thesis, Korea Advanced Institute of Science and Technology, 2008.